ISSN 1063-7834, Physics of the Solid State, 2017, Vol. 59, No. 4, pp. 820–828. © Pleiades Publishing, Ltd., 2017.
Original Russian Text © D.S. Lisovenko, Yu.A. Baimova, L.Kh. Rysaeva, V.A. Gorodtsov, S.V. Dmitriev, 2017, published in Fizika Tverdogo Tela, 2017, Vol. 59, No. 4, pp. 801–809.

ATOMIC CLUSTERS

Equilibrium Structures of Carbon Diamond-Like Clusters and Their Elastic Properties

D. S. Lisovenko[a, *], Yu. A. Baimova[b, c], L. Kh. Rysaeva[b], V. A. Gorodtsov[a], and S. V. Dmitriev[b, d]

[a] *Institute for Problems in Mechanics, Russian Academy of Sciences, Moscow, 119526 Russia*
[b] *Institute for Metal Superplasticity Problems, Russian Academy of Sciences, Ufa, 450001 Bashkortostan, Russia*
[c] *Institute of Metal Physics, Ural Branch, Russian Academy of Sciences, Yekaterinburg, 620990 Russia*
[d] *National Research Tomsk State University, Tomsk, 634050 Russia*
**e-mail: lisovenk@ipmnet.ru*

Received March 21, 2016; in final form, September 7, 2016

Abstract—Three-dimensional carbon diamond-like phases consisting of sp^3-hybridized atoms, obtained by linking of carcasses of fullerene-like molecules, are studied by methods of molecular dynamics modeling. For eight cubic and one hexagonal diamond-like phases on the basis of four types of fullerene-like molecules, equilibrium configurations are found and the elastic constants are calculated. The results obtained by the method of molecular dynamics are used for analytical calculations of the elastic characteristics of the diamond-like phases with the cubic and hexagonal anisotropy. It is found that, for a certain choice of the dilatation axis, three of these phases have negative Poisson's ratio, i.e., are partial auxetics. The variability of the engineering elasticity coefficients (Young's modulus, Poisson's ratio, shear modulus, and bulk modulus) is analyzed.

DOI: 10.1134/S106378341704014X

1. INTRODUCTION

Carbon diamond-like phases (CDPs) consist of carbon atoms each of which has four σ-bonds with neighboring atoms, like in the diamond structure [1]. The lattice of such diamond-like phases is different from the diamond lattice. The base for creation of diamond-like phases may be various polymorphs of carbon: graphene, fullerene-like molecules, and carbon tube structures. Diamond-like phases consisting of fullerene-like molecules have been given the name "fulleranes"; the material consisting of graphene sheets, the name "graphane"; and the material consisting of nanotubes, "tubulan" [1]. Beside nanodiamonds [2], such structures attract much interest from researchers. By now, several carbon diamond-like phases, e.g., polymerized cubic fullerite C_{24} [3, 4] and high-density carbon phase C_8 [5], have been experimentally synthesized and theoretically studied. In a number of theoretical works, the characteristics of different diamond-like phases and their classification are presented in considerable detail [6–9]. In [10], for the first time, it was proposed to construct the nanodiamond phase of covalently bound polymerized nanotubes (4, 0). It was established by calculations that a crystal of polymerized nanotubes must be a semiconductor with a bandgap of 3.18 eV [10]. By methods of molecular dynamics (MD), the structure of carbinoid layers, carbinoid nanotubes, and carbinofullerenes were studied and their basic characteristics were obtained in [11]. The structural characteristics of crystals obtained from polymorphs of graphene were studied in [12]. CDPs and their properties were studied earlier in [13–15]. The equilibrium states of clusters of fullerene-like molecules C_{24} and C_{48} were studied by the MD method in [16, 17].

The most important application of CDPs is the use of them as a covering material for various surfaces: in biomedicine [18], for protection of materials and devices from external actions [19], for wearable materials [20], and for antifriction coatings [21]. Such materials can be produced much more easily and cheaply than diamonds.

The analysis of the elastic properties of single-wall carbon nanotubes has shown that they can have negative Poisson's ratio [22–24]. Many anisotropic nanomaterials of different crystal systems (cubic, hexagonal, tetragonal, etc.) also exhibit negative Poisson's ratio upon stretching in certain directions [25–38]. At the moment, there are more than four hundred materials known to have negative Poisson's ratio (auxetics). More than three hundred of such auxetics have cubic anisotropy [25, 37]. Earlier, the analysis of the elastic constants of some diamond-like phases and fullerite was performed [39–42]. The elastic modules of single-

crystalline C_{60} were determined from measurements of the speed of ultrasound and found to be on the order of $c_{11} \sim 15$ GPa, $c_{12} \sim 9$ GPa, and $c_{44} \sim 6$ GPa [39]; their relaxation contribution [40] and the temperature behavior [41, 42] of their elastic moduli were also analyzed. The bulk moduli of diamond-like phases from fullerene-like molecules were calculated in [13]. It was shown that the bulk moduli vary from 141.2 to 350.5 GPa, which is smaller than the bulk modulus of cubic diamond. The structural and energetic characteristics of different diamond-like phases have been actively investigated in recent years, but many their properties remain insufficiently studied and require further research.

In this paper, we consider diamond-like phases with the cubic, hexagonal, and tetragonal anisotropy, the equilibrium state of which is studied by the MD method. The data obtained by the atomistic simulation are used for the analysis of the elastic characteristics.

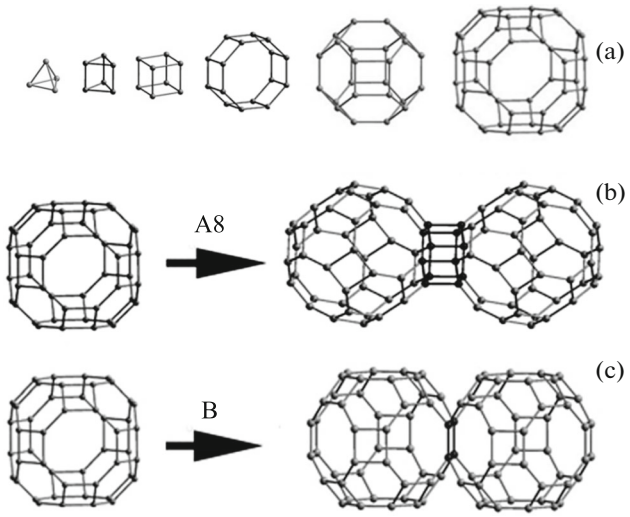

Fig. 1. (a) Fullerene-like molecules C_4, C_6, C_8, C_{16}, C_{24}, and C_{48} (from left to right) and (b, c) two ways of linking of fullerene-like molecules into a cluster.

2. METHODS OF SIMULATION

Stable CDPs were discussed in [1]; leaning upon the computations presented in [1], in this paper, we study diamond-like phases consisting of fullerene-like molecules. According to [1, 13], the same fullerene can be used to create different diamond-like phases, because methods of linking of molecules may be different. The structures are named according to the method of linking of two fullerenes. For instance, the structure denoted by A is formed by linking with covalent bonds and the structure B is obtained by uniting of carbon atoms (Fig. 1). The initial parameters of the diamond-like phases CA1, CA2, CA3, CA4, CA5, CA6, CA7, CA8, CA9, and CB are presented in [1, 13]. Fullerene-like molecules from which the structures under consideration are formed are presented in Fig. 1a: C_4, C_6, C_8, C_{16}, C_{24}, and C_{48}. Eight of ten CDPs with fullerene-like molecules considered here (CA1, CA3, CA4, CA6, CA7, CA8, CA9, CB) have cubic anisotropy, the phase CA2 has hexagonal anisotropy, and the phase CA5 has tetragonal anisotropy [1].

To obtain equilibrium structures of diamond-like phases and estimate their characteristics, we used the LAMMPS software package for MD simulation [43], in which the interatomic interaction is described by the AIREBO potential [44]. In this potential, the binding energy is defined as

$$E_b = \sum_j \sum_{j(j>1)} [V_R(r_{ij}) - \bar{B}_{ij} V_A(r_{ij})], \quad (1)$$

where r_{ij} is the distance between atoms i and j, $\bar{B}_{ij}$ is an empiric function defined in [45], and V_R and V_A are the functions responsible for attraction and repulsion. The functions V_R and V_A are defined by the expressions

$$V_R(r_{ij}) = \frac{D^{(e)}}{S-1} e^{-\sqrt{2S}\beta(r_{ij}-R^{(e)})} f_c(r_{ij}),$$
$$V_A(r_{ij}) = \frac{D^{(e)}S}{S-1} e^{-\sqrt{2S}\beta(r_{ij}-R^{(e)})} f_c(r_{ij}), \quad (2)$$

where the quantities $D^{(e)}$, S, β, $R^{(e)}$ and the function f_c were defined in [45].

This potential has shown good results in the simulation of carbon and hydrocarbon structures, it reproduces well the properties of the covalent bond between two carbon atoms, and is widely used to simulate single- and multilayered graphene sheets [46, 47], crumpled graphene [48, 49], fullerenes [50], etc. The data obtained with this potential are in a good agreement with experimental results and ab initio calculations.

To obtain the equilibrium state of the diamond-like phases under consideration, the minimization of the energies with subsequent relaxation were performed. The relaxation of the system was performed by means of a Nosé–Hoover thermostat. Newton's equations of atomic motion were integrated by the fourth-order Verlet algorithm. Then the compliance coefficients s_{ij} and stiffness coefficients c_{ij} were calculated. To this end, a small uniform strain with one nonzero component was applied to the simulation cell and the resulting stresses were calculated. These stresses were substituted into Hooke's law to calculate the sought-for constants.

3. RESULTS OF SIMULATION

3.1. Equilibrium Structures

Examples of equilibrium phases from clusters of diamond-like molecules can be found in [1, 13] and, therefore, they are not presented here. Below, diamond-like phases are described for the ten aforementioned structures by the method of relaxation to the state with the minimum energy. To calculate the compliance coefficients s_{ij}, a stress linearly increasing in time, with one nonzero component, was applied to the simulation cell and the resulting strains were determined. It turned out that, for strains smaller than 2%, the stress–strain curves are practically linear; from the slopes of these curves, the sought-for constants s_{ij} were calculated from Hooke's law.

For a cubic crystal, it is sufficient to calculate only three compliance coefficients from the expression

$$\begin{pmatrix}\varepsilon_1\\ \varepsilon_2\\ \varepsilon_3\\ \varepsilon_4\\ \varepsilon_5\\ \varepsilon_6\end{pmatrix} = \begin{pmatrix}s_{11} & s_{12} & s_{12} & 0 & 0 & 0\\ s_{12} & s_{11} & s_{12} & 0 & 0 & 0\\ s_{12} & s_{12} & s_{11} & 0 & 0 & 0\\ 0 & 0 & 0 & s_{44} & 0 & 0\\ 0 & 0 & 0 & 0 & s_{44} & 0\\ 0 & 0 & 0 & 0 & 0 & s_{44}\end{pmatrix}\begin{pmatrix}\sigma_1\\ \sigma_2\\ \sigma_3\\ \sigma_4\\ \sigma_5\\ \sigma_6\end{pmatrix}. \quad (3)$$

Here we assume the correspondence $\varepsilon_{xx} \to \varepsilon_1$, $\varepsilon_{yy} \to \varepsilon_2$, $\varepsilon_{zz} \to \varepsilon_3$, $2\varepsilon_{yz} \to \varepsilon_4$, $2\varepsilon_{xz} \to \varepsilon_5$, $2\varepsilon_{xy} \to \varepsilon_6$, $\sigma_{xx} \to \sigma_1$, $\sigma_{yy} \to \sigma_2$, $\sigma_{zz} \to \sigma_3$, $\sigma_{yz} \to \sigma_4$, $\sigma_{xz} \to \sigma_5$, $\sigma_{xy} \to \sigma_6$; s_{11}, s_{12}, and s_{44} are the matrix compliance coefficients of a cubic crystal. For hexagonal anisotropy, Hooke's law reads

$$\begin{pmatrix}\varepsilon_1\\ \varepsilon_2\\ \varepsilon_3\\ \varepsilon_4\\ \varepsilon_5\\ \varepsilon_6\end{pmatrix} = \begin{pmatrix}s_{11} & s_{12} & s_{13} & 0 & 0 & 0\\ s_{12} & s_{11} & s_{13} & 0 & 0 & 0\\ s_{13} & s_{13} & s_{33} & 0 & 0 & 0\\ 0 & 0 & 0 & s_{44} & 0 & 0\\ 0 & 0 & 0 & 0 & s_{44} & 0\\ 0 & 0 & 0 & 0 & 0 & s_{66}\end{pmatrix}\begin{pmatrix}\sigma_1\\ \sigma_2\\ \sigma_3\\ \sigma_4\\ \sigma_5\\ \sigma_6\end{pmatrix}, \quad (4)$$

where s_{11}, s_{33}, s_{44}, s_{12}, s_{13}, and $s_{66} = 2(s_{11} - s_{12})$ are the matrix compliance coefficients of a hexagonal crystal.

The stiffness coefficients for phases with cubic anisotropy were calculated with allowance for the compliance coefficients as follows:

$$c_{11} + c_{12} = \frac{s_{11}}{(s_{11} - s_{12})(s_{11} + s_{12})},$$
$$c_{11} - c_{12} = \frac{1}{s_{11} - s_{12}}, \quad c_{44} = \frac{1}{s_{44}}, \quad (5)$$

Table 1. Compliance coefficients s_{ij} and stiffness coefficients c_{ij} for carbon diamond-like structures with cubic anisotropy

CDP	s_{11}, TPa^{-1}	s_{44}, TPa^{-1}	s_{12}, TPa^{-1}	c_{11}, GPa	c_{44}, GPa	c_{12}, GPa
CA3	1.87	2.496	−0.44	625	401	192
CA4	1.87	9.64	−0.437	624	104	190
CA6	0.948	8.66	−0.072	1068	115	87.8
CA7	8.12	3.64	3.82	455	262	370
CA8	1.67	5.91	−0.299	650	169	142
CA9	3.73	7.31	−0.90	316	137	101
CB	5.53	10	−2.0	306	99.9	174

and, for phases with hexagonal anisotropy, as

$$c_{11} + c_{12} = \frac{s_{33}}{s}, \quad c_{11} - c_{12} = \frac{1}{s_{11} - s_{12}},$$
$$c_{13} = -\frac{s_{13}}{s}, \quad c_{33} = \frac{(s_{11} + s_{12})}{s}, \quad (6)$$
$$c_{44} = \frac{1}{s_{44}}, \quad c_{66} = \frac{1}{s_{66}},$$

where $s = s_{33}(s_{11} + s_{12}) - 2s_{13}^2 > 0$.

In a similar manner, to improve the obtained elastic coefficients, a different method was applied: a strain linearly increasing in time with one nonzero component was applied to the simulation cell and the resulting stresses were determined. The stiffness coefficients were calculated and, from them, the compliance coefficients. The comparison of the results obtained by the different methods has shown that the first method gives more adequate results. The difference between the results given by seemingly similar methods can be explained by the fact that the CDPs under consideration react differently to different methods of loading. The parameters of more stable CDPs can be considered by any of these methods.

The values obtained for diamond-like phases with cubic anisotropy (CA3, CA4, CA6, CA7, CA8, CA9, and CB) are presented in Table 1. From the similar simulation for hexagonal phase CA2, we have the following values of the compliance coefficients: s_{11} = 2.515 TPa^{-1}, s_{33}=1.92 TPa^{-1}, s_{44}=18.4 TPa^{-1}, s_{12} = 0.0906 TPa^{-1}, s_{13} = –0.3625 TPa^{-1}, and s_{66} = 5.94 TPa^{-1}. Using the relationship between the compliance and stiffness coefficients, we obtain c_{11} = 409 GPa, c_{33} = 550 GPa, c_{44} = 54.4 GPa, c_{12} = −3.705 GPa, c_{13} = 76.5 GPa, and c_{66} = 168 GPa. The deformation of the CA5 structure revealed its instability. Even a small (within 0.01%) strain leads to restructuring with the disruption of some bonds. Similarly phase CA1 exhibited its low stability in dynamic conditions. The elastic coefficients obtained for this phase

are not consistent with reality, and the obtainment of consistent results requires additional studies.

3.2. Elastic Properties

On the basis of the values of the compliance coefficients for CDPs with cubic or hexagonal anisotropy, the variability of the elastic engineering coefficients (Young's modulus, Poisson's ratio, shear modulus) was analyzed. Young's modulus, Poisson's ratio, and the shear modulus for anisotropic materials vary with variation in the orientation of the axis of stretching with respect to the crystallographic axes. In the case of linear elasticity, Young's modulus $E(\mathbf{n})$ and Poisson's ratio $\nu(\mathbf{n}, \mathbf{m})$ depend on the tensor compliance coefficients s_{ijkl}, the unit vector $\mathbf{n}$ in the direction of the axis of stretching, and the unit vector $\mathbf{m}$ perpendicular to the direction of stretching [51]:

$$\frac{1}{E(\mathbf{n})} = s_{ijkl} n_i n_j n_k n_l, \tag{7}$$

$$\nu(\mathbf{n}, \mathbf{m}) = -\frac{s_{ijkl} m_i m_j n_k n_l}{s_{\alpha\beta\lambda\mu} n_\alpha n_\beta n_\lambda n_\mu}. \tag{8}$$

The shear modulus $G(\mathbf{n}, \mathbf{m})$ is determined by the unit vector $\mathbf{n}$ normal to the slip plane and the unit vector $\mathbf{m}$ in the slip direction [51]:

$$G^{-1}(\mathbf{n}, \mathbf{m}) = 4 s_{ijkl} n_i m_j n_k m_l. \tag{9}$$

Henceforward, the variability of the engineering elastic coefficients will be described by three Euler's angles: φ, θ, and ψ.

The elasticity of cubic crystals is characterized by three independent matrix compliance coefficients: s_{11}, s_{12}, and s_{44}. Then, Young's modulus, Poisson's ratio, and the shear modulus can be written in the form [37, 52]

$$\frac{1}{s_{11} E} = 1 - \frac{\delta}{2} M(\varphi, \theta), \tag{10}$$

$$\frac{\nu}{s_{11} E} = -\frac{\delta}{2}[N(\varphi, \theta, \psi) - \Pi], \tag{11}$$

$$\frac{1}{s_{44} G} = 1 + (A - 1) N(\varphi, \theta, \psi), \tag{12}$$

$$\Pi \equiv -\frac{2 s_{12}}{\Delta}, \tag{13}$$

$$\delta \equiv \frac{\Delta}{s_{11}}, \tag{14}$$

where

$$A \equiv 2\frac{s_{11} - s_{12}}{s_{44}} = 2\frac{c_{44}}{c_{11} - c_{12}},$$

$$0 \le M \equiv \sin^2 2\theta + \sin^4 \theta \sin^2 2\varphi \le \frac{4}{3},$$

Table 2. Extreme values of the Young's modulus and anisotropy parameter Δ

CDP	Δ, TPa^{-1}	$E_{[100]}$, GPa	$E_{[110]}$, GPa	$E_{[111]}$, GPa
CA3	1.06	535	746	**860**
CA4	−2.51	**535**	320	282
CA6	−3.31	**1055**	384	317
CA7	9.85	123	313	**644**
CA8	−0.99	**599**	462	430
CA9	0.98	268	308	**325**
CB	2.53	181	234	**260**

$$0 \le N \equiv 3\sin^2 \theta \cos^2 \theta \cos^2 \psi + (\cos\theta \cos 2\varphi \cos\psi - \sin\psi)^2 \sin^2 \theta \le 1.$$

The combination of the compliance coefficients, $\Delta \equiv s_{11} - s_{12} - 0.5 s_{44}$, is known as the anisotropy parameter for cubic crystals, and A is Zener's elastic anisotropy ratio.

The analysis of Young's modulus (10) enables one to determine three extreme values [53] corresponding to stretching in the directions [100], [110], and [111]:

$$E_{[100]} = \frac{1}{s_{11}}, \tag{15}$$

$$E_{[110]} = \frac{1}{s_{11} - \Delta/2}, \tag{16}$$

$$E_{[111]} = \frac{1}{s_{11} - 2\Delta/3}. \tag{17}$$

The extreme values of Young's modulus depend on the sign of the anisotropy parameter Δ. For cubic crystals with positive anisotropy, $\Delta > 0$, from relationships (15)–(17), we have $E_{[111]} > E_{[110]} > E_{[100]}$. For cubic crystals with negative anisotropy, $\Delta < 0$, the same relationships imply opposite inequalities $E_{[100]} > E_{[110]} > E_{[111]}$. From the values of the elastic constants of equilibrium structures with cubic anisotropy from carbon diamond-like clusters, presented in Table 1, the extreme values of Young's modulus and values of the anisotropy parameter Δ were determined (Table 2). Three of the equilibrium diamond-like phases with a cubic structure (CA4, CA6, and CA8) have negative anisotropy, and four others have positive anisotropy. Maximum Young's coefficients were observed in the phase CA6 (1055 GPa, $\Delta < 0$) upon stretching in the direction [100] and in the phase CA3 (860 GPa, $\Delta > 0$), in the direction [111]. Bold font in Table 2 emphasizes the maximum values of Young's modulus.

Leaning upon the dimensionless parameters Π and δ (see (13), (14)), all cubic crystals can be divided into three types [37]: nonauxetics ($\Pi > 1$, $\delta > 0$ and $\Pi < 0$, $\delta < 0$), partial auxetics ($0 < \Pi < 1$ for $\delta > 0$ and $\delta < 0$), and complete auxetics ($\Pi < 0$, $\delta > 0$ and $\Pi > 1$, $\delta < 0$). Nonauxetics have positive Poisson's ratio for any ori-

Table 3. Extreme values of Poisson's ratio (global maxima and minima ν_{max}, ν_{min} for particular orientations $\nu_{[100],[001]}$, $\nu_{[001],[110]}$, $\nu_{[1\bar{1}0],[110]}$, and $\nu_{(111),[111]}$), Poisson's ratio averaged over all direction, $\langle\nu\rangle$, and dimensionless parameters Π and δ

CDP	Π	δ	ν_{min}	ν_{max}	$\langle\nu\rangle$	$\nu_{[100],[001]}$	$\nu_{[001],[110]}$	$\nu_{[1\bar{1}0],[110]}$	$\nu_{(111),[111]}$
CA3	0.83	0.57	−0.07	0.33	0.15	0.24	0.33	−0.07	0.07
CA4	−0.348	−1.34	0.14	0.54	0.32	0.23	0.14	0.54	0.36
CA6	−0.044	−3.49	0.03	0.66	0.31	0.08	0.03	0.66	0.37
CA7	0.739	1.21	−0.40	1.14	0.38	0.45	1.14	−0.40	0.23
CA8	−0.606	−0.59	0.14	0.37	0.24	0.18	0.14	0.37	0.27
CA9	1.840	0.26	0.13	0.28	0.21	0.24	0.28	0.13	0.19
CB	1.584	0.46	0.17	0.47	0.33	0.36	0.47	0.17	0.30

entation, and complete auxetics have negative Poisson's ratio. Partial auxetics can have both positive and negative Poisson's ratios. Calculations of the dimensionless parameters Π and δ show that two of the eight considered equilibrium diamond-like structures with cubic anisotropy, CA3 (Π = 0.83) and CA7 (Π = 0.739), can have negative Poisson's ratio (Table 3), i.e., these diamond-like phases are partial auxetics. No complete auxetics have been found among the given diamond-like structures. In addition to the dimensionless parameters Π and δ, Table 3 presents the global maximum and minimum values of Poisson's ratio (ν_{max}, ν_{min}) and Poisson's ratio averaged over all directions, $\langle\nu\rangle$. Minimum Poisson's ratio is observed in the equilibrium structure CA7 ($\nu_{min} = -0.4$). This auxetic has a wide range of the Poisson's ratio ($\nu_{max} - \nu_{min} = 1.54$). Mean Poisson's ratio $\langle\nu\rangle$ for all given crystalline materials proves to be positive and ranging from 0.15 to 0.38. Let us also estimate Poisson's ratio for some special orientations, defined by the formulas

$$\nu_{[100],[001]} = -\frac{s_{12}}{s_{11}}, \quad (18)$$

$$\nu_{[001],[110]} = -\frac{s_{12}}{s_{11} - 0.5\Delta}, \quad (19)$$

$$\nu_{[1\bar{1}0],[110]} = -\frac{2s_{12} + \Delta}{2s_{11} - \Delta}, \quad (20)$$

$$\nu_{(111),[111]} = -\frac{3s_{12} + \Delta}{3s_{11} - 2\Delta}. \quad (21)$$

The last three numbers in brackets indicate the directions of stretching, and the first three numbers in brackets indicate the direction of the lateral strain. Poisson's ratios can be expressed in terms of the dimensionless parameters Π and δ:

$$\nu_{[100],[001]} = \frac{\Pi\delta}{2}, \quad (22)$$

$$\nu_{[001],[110]} = \frac{\Pi\delta}{2 - \delta}, \quad (23)$$

$$\nu_{[1\bar{1}0],[110]} = \frac{\delta(\Pi - 1)}{2 - \delta}, \quad (24)$$

$$\nu_{(111)[111]} = \frac{\delta(1.5\Pi - 1)}{3 - 2\delta}. \quad (25)$$

The consideration of these formulas with using thermodynamic restrictions $\Pi\delta > 2\delta - 2$ and $1 > \Pi\delta > -2$, $\delta < 1.5$ [37] shows that

for $\Pi > 0$ and $0 < \delta < 1.5$

$$\nu_{[001],[110]} > \nu_{[100],[001]} > \nu_{(111)[111]} > \nu_{[1\bar{1}0],[110]},$$

for $\Pi > 0$ and $\delta < 0$

$$\nu_{[1\bar{1}0],[110]} > \nu_{(111)[111]} > \nu_{[001],[110]} > \nu_{[100],[001]},$$

for $\Pi < 0$ and $\delta < 0$

$$\nu_{[1\bar{1}0],[110]} > \nu_{(111)[111]} > \nu_{[100],[001]} > \nu_{[001],[110]},$$

for $\Pi < 0$ and $0 < \delta < 1.5$

$$\nu_{[100],[001]} > \nu_{[001,[110]} > \nu_{(111)[111]} > \nu_{[1\bar{1}0],[110]}.$$

As it is seen from Table 3, the values of Poisson's ratio for special orientations in equilibrium diamond-like structures satisfy these inequalities. For structures CA3 and CA7, negative values are observed for the coefficient $\nu_{[1\bar{1}0],[110]}$.

Figure 2 shows the auxeticity surfaces $\nu(\varphi, \theta, \psi) = 0$ for diamond-like phases CA3 and CA7, constructed in the space of Euler's angles with the periods $T_\varphi = \pi/2$, $T_\theta = 2\pi$, and $T_\psi = \pi$. For these phases, the auxeticity takes place inside these surfaces. From these surfaces, one can determine Euler's angles, i.e., the directions of stretching for which negative Poisson's ratio will be observed. As we see from Fig. 2, the maximum auxeticity zone is inherent in the CA7 crystalline material.

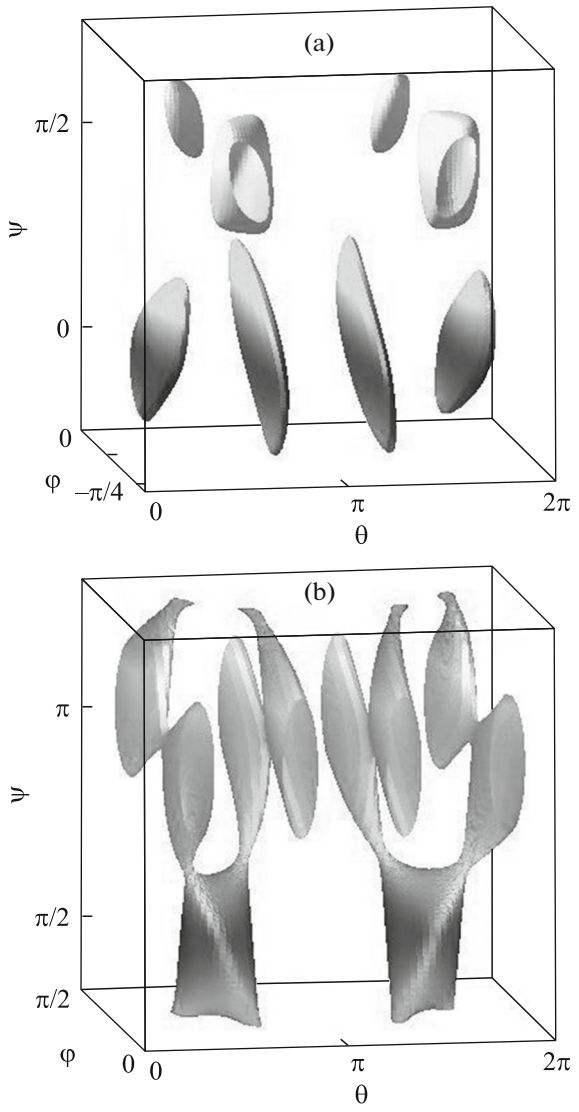

Fig. 2. Auxeticity surfaces of carbon diamond-like structures (a) CA3 and (b) CA7 with cubic anisotropy.

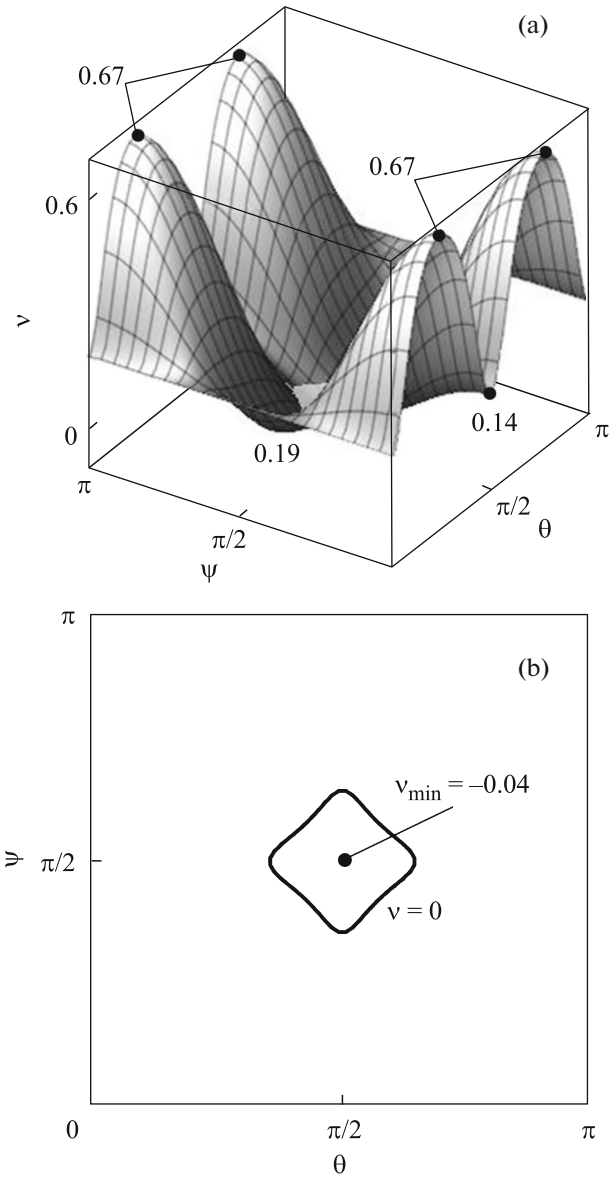

Fig. 3. (a) Surface of Poisson's ratio and (b) auxeticity curve in the space of two Euler's angles for equilibrium diamond-like structure CA2 with hexagonal anisotropy.

The analysis of formula (12) for the shear modulus makes it possible to determine the maximum and minimum values [52]:

$$G_1 = \frac{1}{s_{44}}, \tag{26}$$

$$G_2 = \frac{1}{2(s_{11} - s_{12})}. \tag{27}$$

Which of the extreme values of the shear modulus will be maximal and which the minimal depends on the value of Zener's elastic anisotropy ratio A:

$$A \equiv 2\frac{s_{11} - s_{12}}{s_{44}} = 1 + \frac{2\Delta}{s_{44}}. \tag{28}$$

For cubic crystals with positive anisotropy $\Delta > 0$ (or $A > 1$), relationships (26) and (27) imply $G_1 > G_2$. For cubic crystals with negative anisotropy $\Delta < 0$ (or $0 < A < 1$), we have the opposite inequality: $G_1 < G_2$. Table 4 presents the values of Zener's elastic anisotropy ratio A, extreme values of the shear modulus, and the values of the bulk modulus defined by formula $B = (c_{11} + 2c_{12})/3$. The maximum shear modulus is observed in the diamond-like phase CA6 (490 GPa) at an extreme value of G_2. The minimum shear modulus is observed in structure CA7 ($G_2 = 43$ GPa). The maximum bulk modulus is observed in the equilibrium structure CA6 (415 GPa), and the minimum bulk modulus, in structure CA9 (173 GPa).

Table 4. Maximum and minimum values of shear modulus, Zener's elastic anisotropy ratio A, and bulk modulus B

CDP	A	$G_1 = s_{44}^{-1}$, GPa	$G_2 = (2(s_{11} - s_{12}))^{-1}$, GPa	B, GPa		
				Present work	[1, 8]	[13]
CA3	1.85	400	216	337	342	346.2
CA4	0.48	104	217	335	249	284.5
CA6	0.24	115	490	415	323	350.5
CA7	6.16	262	43	398	207	269.6
CA8	0.67	169	254	311	–	274.5
CA9	1.27	137	108	173	–	239.2
CB	1.50	100	66	218	–	277.6

For hexagonal crystals, Young's modulus (7), Poisson's ratio (8), and shear modulus (9) can be written in the form [54]

$$\frac{1}{E} = s_{11} + (s_{33} - s_{11} - \delta_0 \sin^2\theta)\cos^2\theta, \quad (29)$$

$$-\frac{\nu}{E} = s_{13} + ((s_{12} - s_{13})\sin^2\psi + \delta_0 \cos^2\theta\cos^2\psi)\sin^2\theta, \quad (30)$$

$$\frac{1}{G} = s_{44} + ((2s_{11} - 2s_{12} - s_{44})\sin^2\psi + 4\delta_0 \cos^2\theta\cos^2\psi)\sin^2\theta, \quad (31)$$

$$\delta_0 \equiv s_{11} + s_{33} - 2s_{13} - s_{44}.$$

Young's modulus, shear modulus, and Poisson's ratio under consideration are periodic functions of the angular variables with the periods $T_\theta = T_\psi = \pi$. The engineering elastic coefficients for hexagonal crystals—in contrast to cubic crystals—depend on fewer angles. T he Young's modulus depends on only one Euler's angle (θ), and the shear modulus and Poisson's ratio depend on two angles (θ and ψ).

Figure 3a shows the surface of Poisson's ratio for the diamond-like phase CA2, which proves to be a partial auxetic. The minimum value of Poisson's ratio is obtained upon stretching in the direction [010] and is equal to $\nu_{min} = \nu_{[00\bar{1}],[010]} = -s_{12}/s_{11} = -0.04$. Another extreme value of Poisson's ratio obtained upon stretching in the direction [010] is $\nu_{[100],[110]} = -s_{13}/s_{11} = 0.14$. The maximum value of the Poisson's ratio ($\nu_{max} = 0.67$) is reached at $\theta = 0$ and $\psi = 42°$ and 138°. On stretching in the direction [001], the extreme value of Poisson's ratio is $\nu_{(001),[001]} = -s_{13}/s_{33} = 0.19$. Poisson's ratio averaged over all directions, $\langle\nu\rangle$, takes the value of 0.25. Figure 3b shows the auxeticity curve plotted by the formula

$$s_{13} + ((s_{12} - s_{13})\sin^2\psi + \delta_0 \cos^2\theta\cos^2\psi)\sin^2\theta = 0. \quad (32)$$

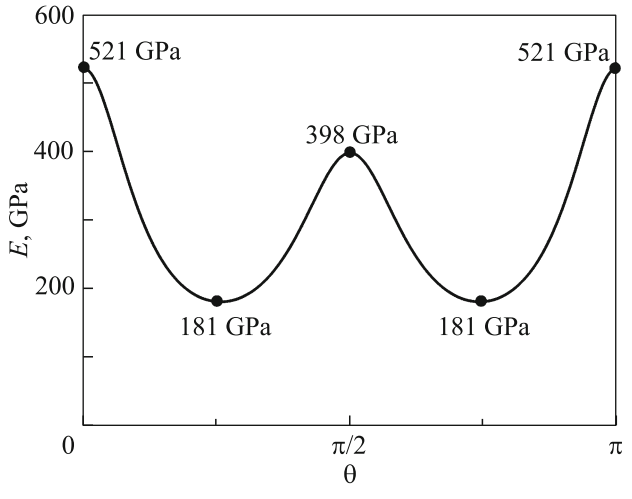

Fig. 4. Variability of Young's modulus of equilibrium diamond-like structure CA2 with hexagonal anisotropy. Dots mark extreme values of Young's modulus.

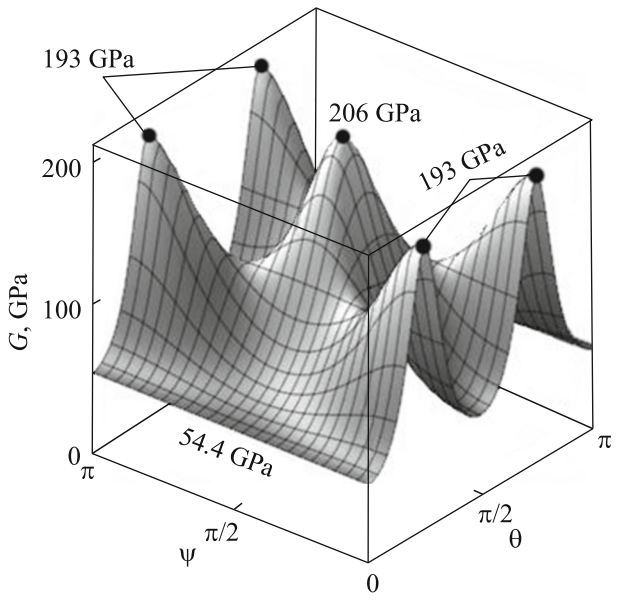

Fig. 5. Surface of the shear modulus equilibrium diamond-like structure CA2 with hexagonal anisotropy.

Table 5. Experimental data (in normal conditions) for cubic diamond

c_{11}, GPa	c_{12}, GPa	c_{44}, GPa	B, GPa	Reference
1079	124	578	442	[59]
1076.4	125.2	577.4	442.3	[60]
1080.4	127	576.6	444.8	[61]
1080.4	127	576.6	443.9	[62]

The auxeticity zone is found inside the domain presented in the figure.

The variability of Young's modulus for the diamond-like structure CA2 is illustrated by Fig. 4, where the extreme values of Young's modulus are also presented. The maximum value of 521 GPa is reached upon stretching in the direction [001]. The minimum value of Young's modulus, $E_{\min} = 181$ GPa, is observed for $\psi = 46°$ and 134°.

The surface of the shear modulus for the diamond-like phase CA2 is shown in Fig. 5. The shear modulus varies from 54.4 GPa at $\theta = 0$ and any ψ, which corresponds to the slip plane (100), to 206 GPa at $\theta = \pi/2$ and $\psi = \pi/2$, which corresponds to the slip plane (010) in the direction [001]. The bulk modulus $B = (2c_{11} + c_{33} + 2c_{12} + 4c_{13})/9$ for the diamond-like phase CA2 is equal to 87.1 GPa. This value proves to be one of smallest when comparing with the bulk coefficients of diamond-like phases with cubic anisotropy (Table 4).

4. CONCLUSIONS

Equilibrium diamond-like phases CA1, CA2, CA3, CA4, CA5, CA6, CA7, CA8, CA9, and CB, obtained by linking of fullerene-like molecules were studied by the molecular dynamics method. Eight of these diamond-like phases (CA1, CA3, CA4, CA6, CA7, CA8, CA9, and CB) are cubic. The structure of CA2 has hexagonal anisotropy, and the structure of CA5 has tetragonal anisotropy. The equilibrium structure CA5 proved to be unstable, the phase CA1 also has low stability, whereas all other phases are stable to a small elastic strain. Calculations of stresses and elastic constants made it possible to analyze other elastic characteristics (Young's modulus, Poisson's ratio, the shear modulus, and the bulk modulus) of diamond-like phases on the basis of clusters of fullerene-like molecules. It has been found the three of the ten diamond-like phases considered—namely, CA2, CA3, and CA7—are auxetics. Since their Poisson's ratio is negative only in definite directions, these structures are partial auxetics. CDPs are novel promising materials of sp^3-hybridized atoms, and this work contributes to the study of their mechanical properties. The search for auxetic materials is an important problem [23, 55–58], because they can be used to develop composite materials with specified elastic properties. In many cases, anomalies of the elastic properties of materials are connected with anomalies of their coefficient of thermal expansion, which is supposed to be calculated in subsequent works.

For comparison, Table 4 presents calculated values of the bulk modulus for the same diamond-like phases, calculated by semiempirical quantum mechanical methods in [1, 8, 13]. We see a substantial quantitative difference between those values and the values of B obtained in the present work by the molecular dynamics method, which apparently is explained by the essential difference between the methods of calculation.

To estimate the mechanical characteristics of the diamond-like phases, obtained above and summarized in Tables 1 and 4, Table 5 presents experimental data for cubic diamond from [59–62]. From the comparison, we can see that the bulk modulus of cubic diamond (~440 GPa) exceeds the bulk coefficients of all diamond-like phases considered here. The minimum difference is observed with the bulk coefficients of the phases CA3, CA6, and CA7. As to the stiffness modulus c_{11}, we observe a surprising proximity of its values for the diamond-like phase CA6 and cubic diamond (Tables 1 and 5).

ACKNOWLEDGMENTS

S.V. Dmitriev acknowledges the support of the Russian Science Foundation, project no. 14-13-00982. Yu.A. Baimova acknowledges the support of the Russian Federation Presidential Scholarship for Young Scientists and Post-Graduate Students no. SP-4037.2015.1. L.Kh. Rysaeva acknowledges the support of the Russian Foundation for Basic Research, project no. 16-32-00483-mol_a.

The analysis of the elastic properties of structures with a cubic anisotropy from carbon diamond-like clusters, performed by D.S. Lisovenko and V.A. Gorodtsov, was supported by the Russian Foundation for Basic Research, project no. 16-01-00325.

REFERENCES

1. V. A. Greshnyakov, E. A. Belenkov, and V. M. Berezin, *Crystal Structure and Properties of Carbon Diamond-Like Phases* (South Ural State University, Chelyabinsk, 2012) [in Russian].
2. V. A. Plotnikov, D. G. Bogdanov, and S. V. Makarov, *Detonation Nanodiamond* (Altai State University, Barnaul, 2014) [in Russian].
3. V. V. Pokropivny and A. V. Pokropivny, Phys. Solid State **46** (2), 392 (2004).
4. V. L. Bekenev and V. V. Pokropivny, Phys. Solid State **48** (7), 1405 (2006).
5. J. Crain, S. J. Clark, G. J. Ackland, M. C. Payne, V. Milman, P. D. Hatton, and B. J. Reid, Phys. Rev. B: Condens. Matter **49** (8), 5329 (1994).
6. E. A. Belenkov and V. A. Greshnyakov, Phys. Solid State **55** (8), 1754 (2013).

7. E. A. Belenkov and V. A. Greshnyakov, Phys. Solid State **57** (1), 205 (2015).
8. V. A. Greshnyakov and E. A. Belenkov, J. Exp. Theor. Phys. **113** (1), 86 (2011)
9. E. A. Belenkov and V. A. Greshnyakov, Phys. Solid State **57** (6), 1253 (2015).
10. H. S. Domingos, J. Phys.: Condens. Matter. **16**, 9083 (2004).
11. E. A. Belenkov and I. V. Shakhova, Phys. Solid State **53** (11), 2385 (2011).
12. E. A. Belenkov and A. E. Kochengin, Phys. Solid State **57** (10), 2126 (2015).
13. E. A. Belenkov and V. A. Greshnyakov, Phys. Solid State **57** (11), 2331 (2015).
14. E. A. Belenkov, M. M. Brzhezinskaya, and V. A. Greshnyakov, Diamond Relat. Mater. **50**, 9 (2014).
15. E. A. Belenkov and V. A. Greshnyakov, J. Exp. Theor. Phys. **119** (1), 101 (2014).
16. R. R. Mulyukov and Yu. A. Baimova, *Carbon Nanomaterials* (Bashkir State University, Ufa, 2015) [in Russian].
17. K. A. Krylova, Yu. A. Baimova, S. V. Dmitriev, and R. R. Mulyukov, Phys. Solid State **58** (2), 394 (2016).
18. R. K. Roy and K.-R. Lee, J. Biomed. Mater. Res. B **83** (1), 72 (2007).
19. X. Li and D. H. C. Chua, in *Ceramic Integration and Joining Technologies: From Macro to Nanoscale*, Ed. by M. Singh, T. Ohji, R. Asthana, and S. Mathur (Wiley, Hoboken, 2011), p. 641.
20. W. I. Milne, Semicond. Sci. Technol. **18**, S81 (2003).
21. J. Robertson, Mater. Sci. Eng., R **37**, 129 (2002).
22. G. Van Lier, C. Van Alsenoy, V. Van Doren, and P. Geerligs, Chem. Phys. Lett. **326**, 181 (2000).
23. F. Scarpa, S. Adhikari, and C. Y. Wang, J. Phys. D: Appl. Phys. **42**, 142002 (2009).
24. A. Smolyanitsky and V. K. Tewary, Nanotechnology **22**, 085703 (2011).
25. R. H. Baughman, J. M. Shacklette, A. A. Zakhidov, and S. Stafstrom, Nature (London) **392**, 362 (1998).
26. S. P. Tokmakova, Phys. Status Solidi B **242**, 721 (2005).
27. A. Norris, Proc. R. Soc. London, Ser. A **462**, 3385 (2006).
28. T. Paszkiewicz and S. Wolski, Phys. Status Solidi B **244**, 966 (2007).
29. T. Paszkiewicz and S. Wolski, J. Phys.: Conf. Ser. **104**, 012038 (2008).
30. A. C. Branka, D. M. Heyes, and K. W. Wojciechowski, Phys. Status Solidi B **246**, 2063 (2009).
31. R. V. Goldshtein, V. A. Gorodtsov, and D. S. Lisovenko, Mech. Solids **45** (4), 529 (2010).
32. R. V. Goldshtein, V. A. Gorodtsov, and D. S. Lisovenko, Dokl. Phys. **56** (7), 399 (2011).
33. A. C. Branka, D. M. Heyes, and K. W. Wojciechowski, Phys. Status Solidi B **248**, 96 (2011).
34. A. C. Branka, D. M. Heyes, Sz. Mackowiak, S. Pieprzyk, and K. W. Wojciechowski, Phys. Status Solidi B **249**, 1373 (2012).
35. R. V. Goldstein, V. A. Gorodtsov, and D. S. Lisovenko, Phys. Status Solidi B **250** (10), 2038 (2013).
36. V. V. Krasavin and A. V. Krasavin, Phys. Status Solidi B **251**, 2314 (2014).
37. R. V. Goldshtein, V. A. Gorodtsov, D. S. Lisovenko, and M. A. Volkov, Phys. Mesomech. **17** (2), 97 (2014).
38. R. V. Gol'dshtein, V. A. Gorodtsov, D. S. Lisovenko, and M. A. Volkov, Lett. Mater. **5** (4), 409 (2015).
39. N. P. Kobelev, R. K. Nikolaev, Ya. M. Soifer, and S. S. Khasanov, Phys. Solid State **40** (1), 154 (1998).
40. N. P. Kobelev, Phys. Solid State **44** (1), 195 (2002).
41. N. P. Kobelev, R. K. Nikolaev, N. S. Sidorov, and Ya. M. Soifer, Phys. Solid State **44** (3), 429 (2002).
42. N. P. Kobelev, R. K. Nikolaev, N. S. Sidorov, and Ya. M. Soifer, Phys. Solid State **43** (12), 2344 (2001).
43. http://lammps.sandia.gov/
44. S. Stuart, A. Tutein, and J. Harrison, J. Chem. Phys. **112**, 6472 (2000).
45. W. Brenner, Phys. Rev. B: Condens. Matter **42**, 9458 (1992).
46. A. K. Singh and R. G. Hennig, Phys. Rev. B: Condens. Matter **87**, 094112 (2013).
47. S. Costamagna, M. Neek-Amal, J. H. Los, and F. M. Peeters, Phys. Rev. B: Condens. Matter **86**, 041408 (2012).
48. J. A. Baimova, B. Liu, S. V. Dmitriev, N. Srikanth, and K. Zhou, Phys. Chem. Chem. Phys. **16**, 19505 (2014).
49. Yu. A. Baimova, R. T. Murzaev, and S. V. Dmitriev, Phys. Solid State **56** (10), 2010 (2014).
50. L. Kh. Rysaeva and Yu. A. Baimova, Fundam. Probl. Sovrem. Materialoved. **12** (4), 439 (2015).
51. Yu. I. Sirotin and M. P. Shaskol'skaya, *Fundamentals of Crystal Physics* (Nauka, Moscow, 1975, Mir, Moscow, 1982).
52. R. V. Goldshtein, V. A. Gorodtsov, and D. S. Lisovenko, Lett. Mater. **2** (1), 21 (2012).
53. R. V. Goldshtein, V. A. Gorodtsov, and D. S. Lisovenko, Lett. Mater. **1** (3), 127 (2011).
54. R. V. Goldshtein, V. A. Gorodtsov, and D. S. Lisovenko, Dokl. Phys. **56** (12), 602 (2011).
55. K. W. Wojciechowski, Phys. Lett. A **137** (1–2), 60 (1989).
56. K. V. Tretiakov and K. W. Wojciechowski, Phys. Status Solidi B **250**, 2020 (2013).
57. J. N. Grima, S. Winczewski, L. Mizzi, M. C. Grech, R. Cauchi, R. Gatt, D. Attard, K. W. Wojciechowski, and J. Rybicki, Adv. Mater. (Weinheim) **27** (8), 1455 (2015).
58. K. L. Alderson, A. Alderson, J. N. Grima, and K. W. Wojciechowski, Phys. Status Solidi B **251** 263 (2014).
59. H. J. McSkimin and P. Andreatch, J. Appl. Phys. **43**, 2944 (1972).
60. M. Grimsditch and A. K. Ramdas, Phys. Rev. B: Solid State **11**, 3139 (1975).
61. E. S. Zouboulis, M. Grimsditch, A. K. Ramdas, and S. Rodrigues, Phys. Rev. B: Condens. Matter **57**, 2889 (1998).
62. A. Migliori, H. Ledbetter, R. G. Leisure, and J. B. Betts, J. Appl. Phys. **104**, 053512 (2008).

Translated by E. Chernokozhin